Islamic University Journal of Applied Sciences (IUJAS)
https://journals.iu.edu.sa/jesc

Volume VIII, Issue II, December 2026, Pages 57-72

Aerodynamic Analysis Using CFD of a Formula SAE Car Front Nose

Faisal Omar Mahroogi [1] *

[1] Department of Mechanical Engineering, Faculty of Engineering, Islamic University of Madinah, Saudi Arabia, f.mahroogi@iu.edu.sa

*Corresponding author: (Faisal O. Mahroogi), *Email Address*: f.mahroogi@iu.edu.sa

Abstract

The aerodynamic performance of Formula SAE (FSAE) cars strongly influences speed, stability, and energy efficiency. This study introduces a systematic CFD based comparison of four front nose geometries an aspect that remains underexplored in existing FSAE literature. Four distinct nose shapes were modeled in SolidWorks and evaluated in ANSYS Fluent under identical boundary conditions at a free stream velocity of 100 km/h. The Reynolds Averaged Navier–Stokes (RANS) equations were solved using the k–ω SST turbulence model, and a mesh independence study ensured numerical accuracy. The optimized nose achieved a drag coefficient of 0.24, representing a 14% reduction relative to the published baseline value of 0.28, thereby quantifying the aerodynamic improvement contributed by this work. Flow field analysis confirmed smoother airflow, delayed separation, and reduced wake turbulence for the optimized geometry. These findings provide new insight into front nose aerodynamic optimization and offer practical design guidance for FSAE teams and potential applications in race car and electric-vehicle aerodynamics.

Keywords: Aerodynamics; Computational Fluid Dynamics (CFD); Drag coefficient; Formula SAE; Front nose; k-ω SST turbulence model.

https://doi.org/10.63070/jesc.2026.034
Received 22 April 2026; Revised 28 May 2026; Accepted 15 May 2026; Available online 20 June 2026.
Published by Islamic University of Madinah on behalf of ***Islamic University Journal of Applied Sciences.***
This is an open access article published under the Creative Commons Attribution 4.0 International license (CC BY 4.0):https://creativecommons.org/licenses/by/4.0/

1. Introduction

Computational Fluid Dynamics (CFD) has emerged as an essential tool in aerodynamic analysis and vehicle design, particularly in high-performance motor-sport applications such as Formula Student (FS) and Formula SAE (FSAE) competitions. CFD combines the principles of fluid mechanics, numerical methods, and computer modeling to predict fluid-flow behavior, including drag, lift, pressure distribution, and wake formation around vehicle components. These capabilities are particularly valuable in FS, where teams of student engineers design, build, and race single-seat formula-style vehicles. Aerodynamics significantly influences the competitiveness of these cars by affecting downforce, drag, fuel efficiency, and overall stability.

Over the past decade, numerous studies have used CFD to optimize the aerodynamic elements of FS and FSAE vehicles. The design of rear wings using three-dimensional CFD has been a prominent research focus, contributing to drag reduction and improved downforce [1]. Broader system-level modeling and analysis have also been undertaken to evaluate the interaction of multiple aerodynamic components [2]. Notably, nose-shape optimization using adjoint methods has proven effective in minimizing drag and directly enhancing speed and fuel economy [3]. Front-wing shape optimization has similarly improved vehicle stability and cornering dynamics [4].

Comprehensive aerodynamic analyses using CFD have extended to external body geometries [5, 6], rear diffusers [13], and spoiler geometries [7, 8], confirming that refined shapes can deliver significant performance gains. Some studies have validated these simulations using experimental techniques and vehicle-dynamics testing [9]. Research on wake behavior [10], front-wing redesign [11], and general vehicle analysis using ANSYS Fluent [12] has highlighted the role of CFD in simulating realistic aerodynamic conditions.

Specific components such as the Gurney flap [14], aerodynamic profiles [15], and spoiler interactions [16] have also been investigated to understand their effects on longitudinal stability. CFD analyses have been applied to the flow around race-car wheels [17], the DrivAer reference model [18], and canards [19] to study localized aerodynamic changes. More recent approaches have combined machine learning with CFD to optimize rear spoilers and enhance lateral stability in passenger and electric vehicles [20].

The placement of rear aerodynamic components has been optimized using CFD for motor-sport applications, for example on the Aston Martin DB7 [21], while the effectiveness of underbody diffusers in road cars has also been validated [22]. Studies integrating structural and aerodynamic design, such as Formula One front-wing assemblies [24], have stressed the importance of a multi-

disciplinary approach. Undertray performance has been optimized for FS cars [25], and component-specific studies on air-intake restrictors [26], flow transitions [27], and high-speed vehicle aerodynamics [28] have further refined the collective understanding. Simulations on body-design variations [29], FSC racing-car bodies [30], and concept sports cars [31] further illustrate the breadth of CFD applications in performance engineering. Finally, investigations of spoiler-induced stability [32] and pitch sensitivity in race-car aerodynamics [33] complete a substantial body of work that underscores the value of precise aerodynamic modeling for vehicle dynamics. Wind-tunnel testing of FS vehicles has likewise been used to verify CFD trends and improve simulation fidelity [23].

Recent advances in Formula Student and FSAE aerodynamics have increasingly focused on detailed CFD based investigations of forward aerodynamic components. Piszczatowski et al. [35] analyzed the front wing cross section of a Formula Student vehicle and demonstrated how subtle geometric variations influence pressure distribution and downforce generation, emphasizing the sensitivity of leading edge components to shape refinement. Building on this component level understanding, Hogea et al. [36] performed a 3D iterative parametric optimization of a complete FSAE aerodynamic package, showing that coordinated adjustments across multiple elements can yield substantial improvements in drag and downforce. These studies collectively highlight the growing reliance on high fidelity CFD workflows to guide aerodynamic decision making in student motorsport engineering.

Parallel developments in turbulence modeling strategies have further strengthened the accuracy of automotive aerodynamic simulations. Sankar et al. [37] compared Detached Eddy Simulation (DES) with traditional RANS approaches, demonstrating that higher fidelity models capture complex flow structures, such as vortex shedding and transient separation, more effectively, particularly around curved or highly loaded surfaces. Complementing this, Telli and Rosa [38] reviewed the aerodynamic influence of front wing geometry in Formula One, underscoring how wing shape modifications affect drag, downforce, and wake behavior. Together, these works establish a strong foundation for focused investigations into forward aerodynamic surfaces and motivate the present study, which extends the literature by evaluating multiple front nose geometries under identical CFD conditions and quantifying their impact on drag, lift, and flow field characteristics.

Despite this extensive work, most published studies have focused on isolated components. There is a notable research gap in fully integrated, front-nose-specific aerodynamic studies within a Formula SAE context. The front nose is the leading interface between the car and the oncoming airflow and plays a critical role in managing pressure gradients, minimizing flow separation, and initiating laminar-to-turbulent transitions.

This study addresses this gap by conducting a CFD-based aerodynamic comparison of four distinct Formula SAE front-nose geometries. By focusing on one of the most aerodynamically sensitive regions of the vehicle and building established methodologies [2, 3, 5, 12, 14, 29], the work identifies the design that provides optimal drag reduction without compromising the lift balance required for stability. The results are expected to deliver practical insights for student engineering teams seeking competitive advantages in Formula SAE through evidence-based aerodynamic refinement.

2. Methodology

2.1 Selection of CFD Tool

ANSYS Fluent was selected as the primary CFD solver for this study. The software is widely recognized as an industry-standard tool, known for its robustness and accuracy in simulating complex aerodynamic environments. It supports a broad range of turbulence models, adaptive meshing techniques, and solver settings that are essential for capturing intricate flow behavior in automotive contexts. The k-ω Shear Stress Transport (SST) turbulence model was chosen because this hybrid formulation blends the near-wall accuracy of the k-ω model with the free-stream robustness of the k-ε model, making it particularly effective at predicting boundary-layer separation and near-wall flow phenomena that directly affect the drag and lift around the vehicle nose.

2.2 Governing Equations

The airflow was modeled using the Reynolds-Averaged Navier–Stokes (RANS) equations, which are suitable for capturing time-averaged turbulent flow over complex geometries. A steady-state solver was employed under the assumption of continuous and consistent race conditions, balancing computational efficiency with a sufficiently detailed representation of aerodynamic behavior. For incompressible flow, mass conservation is enforced through the continuity equation:

$$\frac{\partial \rho}{\partial t} + \nabla \cdot (\rho \mathbf{v}) = 0 \tag{1}$$

where ρ is the fluid density and v is the velocity vector field. Momentum conservation is expressed by the Navier–Stokes equation:

$$\rho \left(\frac{\partial \mathbf{v}}{\partial t} + \mathbf{v} \cdot \nabla \mathbf{v} \right) = -\nabla p + \mu \nabla^2 \mathbf{v} + \mathbf{F} \tag{2}$$

where p denotes pressure, μ is the dynamic viscosity, and F represents body forces per unit volume. Time averaging these equations introduces the Reynolds-stress term, which requires a turbulence-closure model. The k-ω SST model solves two transport equations, one for the turbulent kinetic energy k and one for the specific dissipation rate ω:

$$\frac{\partial k}{\partial t} + \mathbf{v} \cdot \nabla k = P_k - \beta k\omega + \nabla \cdot [(\nu + \sigma_k \nu_t)\nabla k] \quad (3)$$

$$\frac{\partial \omega}{\partial t} + \mathbf{v} \cdot \nabla \omega = \frac{\alpha}{\nu_t} P_k - \beta \omega^2 + \nabla \cdot [(\nu + \sigma_\omega \nu_t)\nabla \omega] \quad (4)$$

where P_k is the production of turbulent kinetic energy, ν is the kinematic viscosity, ν_t is the turbulent (eddy) viscosity, and σ_k, σ_ω, β, β^*, and α are standard model constants. The k-ω SST model is particularly effective in predicting flow separation and boundary-layer development, both of which are critical to estimating drag and optimizing the aerodynamic performance of the front nose.

2.3 Aerodynamic Force Coefficients

The drag force F_d acting on the car is a primary outcome of the simulations and is related to the drag coefficient C_d through:

$$F_d = \frac{1}{2}\, \rho\, v^2\, C_d\, A \quad (5)$$

where v is the free-stream velocity relative to the car, *Cd* is the dimensionless drag coefficient, and A is the frontal reference area of the vehicle. This relation allows a quantitative comparison between different nose geometries through their drag coefficients, which directly influence top speed and fuel consumption. Similarly, the lift coefficient C_l is evaluated to assess any lift (or downforce) generated by the nose design:

$$C_l = \frac{2L}{\rho\, v^2\, A} \quad (6)$$

where L is the lift force; for race cars, negative values (downforce) are generally desirable. The lift coefficient is essential for assessing vehicle stability, since excessive lifts reduce tire grip while appropriate downforce improves handling and cornering.

2.4 Computational Domain and Boundary Conditions

A structured computational domain was constructed to replicate realistic flow conditions and to eliminate artificial effects from the proximity of the outer boundaries. The domain extends ten vehicle lengths in the streamwise direction, five vehicle widths laterally, and five vehicle heights vertically. This generous sizing ensures that the boundary conditions do not interfere with the flow near the vehicle and that the wake can fully develop before reaching the outlet.

The boundary conditions were selected to mimic a representative racing scenario. At the inlet, a uniform velocity of 100 km/h (approximately 27.8 m/s) was applied, representative of the average track speed during an FSAE event. This velocity corresponds to a length-based Reynolds number of approximately 1.2×10^6, confirming that the flow regime is fully turbulent. At the outlet, a pressure boundary condition of 0 Pa Gauge was imposed to allow the air to exit the domain freely and to emulate an open atmospheric environment. The ground was modeled as a moving wall translating at the same speed as the inlet flow (100 km/h) with a no-slip condition, correctly simulating the relative motion between the vehicle and the track surface. A no-slip condition was also applied to the vehicle surface itself, which is essential for resolving wall shear stress, pressure distribution, and boundary-layer development.

2.5 Mesh Generation and Independence Study

An unstructured tetrahedral mesh was used to capture the complex geometry of the car, including the nose, suspension arms, and undertray. Mesh refinement was applied in critical regions such as the nose surface, underbody, wheel arches, and near-wake zones to resolve the sharp gradients in pressure and velocity. To accurately capture near-wall flow, prism layers were added to form a boundary-layer mesh. The first cell height was selected to keep y^+ values in the range of 30–100, which is suitable for the k-ω SST model without requiring full wall resolution.

A mesh-independence study was carried out by successively refining the mesh density and monitoring the variations in drag (C_d) and lift (C_l) coefficients. Refinement continued until the change in both coefficients between successive mesh levels was less than 1%, confirming mesh independence. The final mesh consisted of approximately 25 million cells, providing a suitable balance between accuracy and computational feasibility.

2.6 Convergence Criteria and Stability

Convergence was considered to be achieved when both numerical and physical criteria were satisfied. The scaled residuals for the continuity equation, the three momentum components, the turbulent kinetic energy (k), and the specific dissipation rate (ω) all had to drop below 10^{-5}. In addition, the drag and lift coefficients had to stabilize, with variations of less than 0.1% between successive iterations, indicating that a steady-state solution had been reached. Under-relaxation factors and multigrid acceleration were used to improve numerical stability and to reduce the iteration count without compromising accuracy. After convergence, the velocity and pressure fields were inspected for physical realism; the absence of unphysical spikes or reversed flow confirmed the reliability of the numerical solution.

2.7 Nose Design

Four distinct nose geometries were designed in SolidWorks and subjected to identical boundary conditions in ANSYS Fluent to allow direct comparison. The four candidate shapes are illustrated in Fig. 1. The complete vehicle model, including wheels, suspension, and underbody components, was prepared in SolidWorks and then exported to ANSYS Meshing for discretization prior to the CFD analysis.

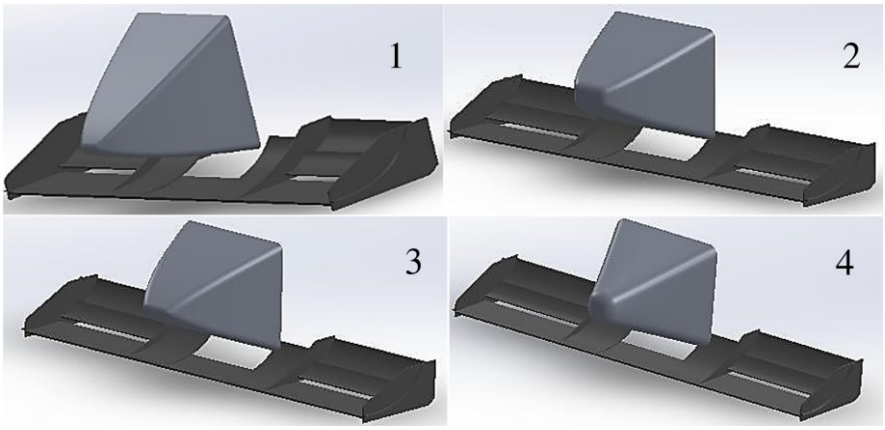


Figure 1. The four-candidate nose-shape models used in the CFD study.

3. Results and Discussion

3.1 Aerodynamic Coefficients for the Four Candidate Noses

The four candidate nose geometries were evaluated under identical boundary conditions at a free-stream velocity of 100 km/h. Table I summarizes the drag coefficient C_d, drag force F_d, lift coefficient C_l, and lift force L extracted from the converged CFD solutions.

Table I. Aerodynamic coefficients and forces obtained from CFD for the four nose shapes at a free-stream velocity of 100 km/h.

Shape #	**Drag coefficient C_d**	**Drag force F_d (N)**	**Lift coefficient C_l**	**Lift force L (N)**
1	0.24	71.906	0.0332	34.84
2	0.27	79.430	0.0522	54.27
3	0.26	76.507	0.0418	43.46
4	0.25	75.047	0.0354	36.81

Shape 1 produced the lowest drag coefficient (C_d = 0.24) and the lowest lift coefficient (C_l = 0.0332), which corresponds to a modest lift force of 34.84 N. Shape 2 exhibited the highest drag and the highest lift, making it the least favorable configuration from an aerodynamic-efficiency standpoint. Shapes 3 and 4 fell between these extremes, with Shape 4 performing only marginally worse than Shape 1 in drag. On this basis, Shape 1 was selected as the optimized design. Its low drag coefficient is expected to translate into higher achievable top speeds and reduced fuel consumption during FSAE dynamic events.

3.2 Flow-Field Analysis

Velocity contours and streamline plots were generated for each candidate geometry to visualize how the flow interacts with the different nose shapes. For the selected (optimized) geometry, the velocity contours show a smooth flow over the forward surface and delayed separation along the sides and top of the nose, consistent with the low drag coefficient observed in Table I. Pressure-coefficient (*Cp*) plots indicate a more uniform pressure distribution and a reduced stagnation peak, which results in lower pressure drag and a more aerodynamic profile. Streamline visualizations confirm that the wake behind Shape 1 is smaller and less turbulent than the wakes of the other three geometries, whose flow separation begins earlier along the nose and produces larger, more energetic trailing structures. Figs. 2 and 3 illustrate, respectively, the two-dimensional streamline contour in the z-direction and the z-directional velocity field for the optimized geometry.

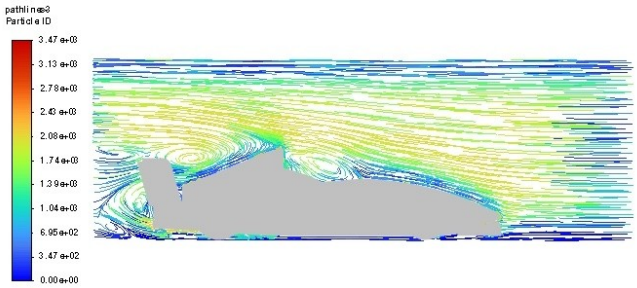


Figure 2. CFD two-dimensional contour of the z-directional streamlines around the vehicle.

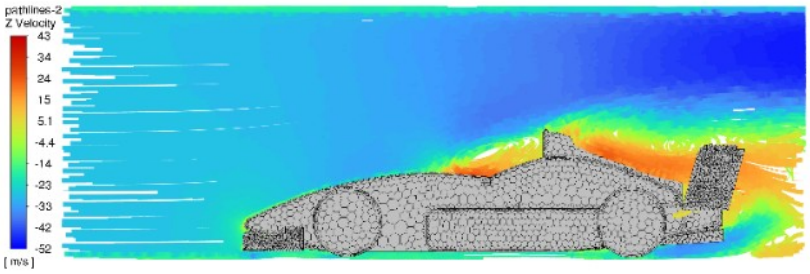


Figure 3. CFD visualization of the velocity field in the z-direction for the optimized geometry (Shape 1).

Iterative testing of the parametric design space highlighted two consistent trends. First, a shorter, more rounded nose profile (as in Shape 1) reduces the frontal area and improves flow attachment, yielding approximately a 3.5% drag reduction relative to the longer alternatives. Second, a more tapered cross-section reduces pressure drag and turbulence while keeping the generated lift within the acceptable range for overall vehicle balance. The final nose geometry therefore represents a balanced compromise between drag reduction and vehicle control, both of which are vital in competitive racing.

3.3 Comparative Analysis

The results were compared with previous CFD studies and empirical data to validate the findings. The drag coefficient of 0.24 obtained for the optimized nose corresponds to approximately a 14% reduction relative to the reference value of 0.28 reported for baseline FSAE configurations with conventional front-nose geometries [12]. This reduction is consistent with the 10–15% improvements documented in [3] and [15] for streamlined nose profiles, supporting the effectiveness of the design refinements adopted in this study.

Flow-visualization results show that the rounded geometry delays separation and reduces wake size, which matches the findings of [14] and other prior studies where angular nose designs produced more turbulent wakes. These flow-field improvements contribute directly to the lower drag, as confirmed by the streamline and velocity-contour plots in Figs. 2 and 3.

When compared with published wind-tunnel data [23], the present drag coefficient is slightly lower than the 0.26 observed experimentally for moderately optimized FSAE configurations. This small difference is expected, as CFD assumes idealized conditions, smooth surfaces, perfect symmetry, steady-state operation, whereas real-world tests include surface imperfections, mounting-hardware interference, and environmental variability. The optimized lift coefficient ($C_l = 0.033$) also falls within the typical empirical range of 0.03-0.05 reported in the literature, confirming the capacity of the design to maintain adequate downforce for vehicle stability. The pressure-distribution trends further validate

this, matching the general patterns reported in the experimental literature. Overall, the CFD results agree closely with both prior simulations and physical benchmarks, reinforcing the reliability of the model. Future work should incorporate dedicated wind-tunnel validation to further confirm the aerodynamic performance under actual operating conditions.

3.4 Practical Implications

The aerodynamic optimization of the front nose demonstrated in this study offers direct performance benefits for Formula SAE vehicles. The reduction in drag enhances acceleration, top speed, and energy efficiency, all of which are critical in competitive racing. Maintaining a balanced lift coefficient also preserves vehicle stability and improves tire grip during aggressive maneuvers. Teams can leverage the parametric design approach presented here to adapt nose geometries to their specific vehicle configurations and extend similar techniques to other aerodynamic components such as rear wings or undertrays.

Beyond racing, these findings are relevant to production vehicles, particularly electric and hybrid cars, where minimizing aerodynamic drag improves range and reduces noise emissions. The smoother airflow and smaller wake associated with the optimized nose also help mitigate aerodynamic noise, which is increasingly perceptible in quiet electric powertrains. Finally, the study highlights the role of CFD as a cost-effective alternative to physical prototyping: by using simulation during early development, teams and manufacturers can reduce reliance on expensive wind-tunnel models, shorten design cycles, and iterate geometries more freely. The project also serves as an educational example, engineering students can use its methodology to understand the practical application of fluid dynamics and vehicle design with modern simulation tools. The final fabricated Formula SAE vehicle is shown in Fig. 4.



Figure 4. Final fabricated Formula SAE car.

4. Conclusions

This study optimized the aerodynamic performance of a Formula SAE car's front-nose geometry using CFD simulations in ANSYS Fluent with the k-ω SST turbulence model. Four candidate nose shapes were modeled in SolidWorks and evaluated under identical boundary conditions at 100 km/h. Among the tested designs, the optimized nose (Shape 1) achieved a 14% reduction in drag coefficient relative to the baseline reference, without compromising the lift balance and therefore preserving the downforce required for high-speed handling and cornering stability.

Flow-field analyses revealed smoother airflow, delayed flow separation, and reduced wake formation around the optimized geometry. A more uniform pressure distribution on the forward surface further confirms its aerodynamic efficiency, and these characteristics directly explain the reduction in pressure drag, a key factor in overall performance.

Although the results align with existing simulation benchmarks and published experimental data, empirical validation through wind-tunnel testing remains desirable. Steady-state RANS simulations necessarily rely on idealizations, smooth surfaces, perfect symmetry, steady inflow, that may not fully reflect real-world conditions, and dedicated experiments would help identify any discrepancies due to surface imperfections or environmental effects.

The practical implications of this research extend beyond FSAE competitions. The parametric design and optimization workflow presented here is directly transferable to broader automotive applications,

including electric and hybrid vehicles, where aerodynamic efficiency strongly influences energy consumption and driving range. The methodology also illustrates how CFD can act as a cost-effective alternative to early-stage physical prototyping.

The study is limited to the front nose and does not account for aerodynamic interactions with other components such as rear wings and diffusers. Computational resources also constrained the use of higher-order solvers and transient simulations, which are needed to capture dynamic effects during parking or cornering. Recommended future work therefore includes: (i) wind-tunnel testing to validate and refine the CFD models; (ii) expansion of the simulations to full-vehicle aerodynamics; (iii) incorporation of transient flow simulations for dynamic analysis; (iv) study of material and manufacturing tolerance effects on aerodynamic performance; and (v) exploration of advanced optimization techniques, including machine learning and genetic algorithms.

In conclusion, this research successfully delivered a front-nose design that enhances aerodynamic efficiency while maintaining vehicle stability. The findings contribute both to academic understanding and to the practical development of high-performance vehicles, offering a replicable approach for future aerodynamic-optimization efforts in motorsport and general automotive engineering. The optimized nose (Shape 1) achieved a drag coefficient of 0.24, representing a 14% reduction compared to the baseline value of 0.28.

References

[1] Dharmawan, M. A., Tjahjana, D. D. P., Kristiawan, B., and Pertiwi, S. I., "Design and Aerodynamics Analysis of Rear Wing Formula Student Car Using 3-Dimension CFD (Computational Fluid Dynamics)." *AIP Conference Proceedings* 2217, no. 1 (2020). https://doi.org/10.1063/5.0001049

[2] Baren, I. V., Milligan, A. V., Ashcraft, S., Rosser, S., and Wang, X., "Modeling, Analysis and Design of the Formula SAE Aerodynamics System." In *Proceedings of the ASME International Mechanical Engineering Congress and Exposition*, vol. 84584, V010T10A062, 2020. https://doi.org/10.1115/IMECE2020-24374

[3] Hoque, M. A., Rahman, M. S., Rimi, K. N., Alif, A. R., and Haque, M. R., "Enhancing Formula Student Car Performance: Nose Shape Optimization via Adjoint Method." *Results in Engineering* 20 (2023): 101636. https://doi.org/10.1016/j.rineng.2023.101636

[4] Kalinowski, M. and Szczepanik, M., "Aerodynamic Shape Optimization of Racing Car Front Wing." *IOP Conference Series: Materials Science and Engineering* 1037, no. 1 (2021): 012058. https://doi.org/10.1088/1757-899X/1037/1/012058

[5] G. V. Kulkarni, H. S. Balasubramanya, B. V. Nagesh, Y. Lakkegowda, and B. R. Omkaresh, "Aerodynamics study of the Formula SAE car using analytical approach," Journal of Mines, Metals & Fuels, vol. 70, no. 4, pp. 455–461, 2022. https://doi.org/10.18311/jmmf/2022/32024

[6] A. Mohanan, J. A. Pandey, A. V. Gupta, S. G. Almeida, and D. Choudhari. "Development of External Aerodynamics of an FSAE Racecar Using Computational Fluid Dynamics.", *International Journal of Engineering Research & Technology (IJERT)*, 2021. ISSN: 2278-0181

[7] S. Patil, and L. B. Rao. "Aerodynamic Study of the Different Spoiler Section Design Used in Formula-SAE Cars." *SAE Technical Paper* 2021-28-0181, 2021. https://doi.org/10.4271/2021-28-0181

[8] S. Wille, K. Hendrickson, and R. K. Agarwal. "Optimization Study of Front and Rear Wings of Motorsport Using Computational Fluid Dynamics." In *AIAA SciTech 2021 Forum*, 1734, 2021. https://doi.org/10.2514/6.2021-1734

[9] E. S. Cole, "*Design and Validation of an Aerodynamic System for a Formula SAE Vehicle Using Vehicle Dynamic Simulation and Experimentation."* Master's thesis, West Virginia University, 2023.

[10] A. Guerrero, and R. Castilla, "Aerodynamic Study of the Wake Effects on a Formula 1 Car." *Energies* 13, no. 19 (2020): 5183. https://doi.org/10.3390/en13195183

[11] Bavapuram, V. S. S., S. N. Suresh, S. Sharma, and V. Kaushik, "Aerodynamic Performance Analysis of Formula-Based Vehicle Through ANSYS." In *Future Learning Aspects of Mechanical Engineering*, 121–132. Singapore: Springer, 2022.

[12] Md. Hassaan, S. Dewivedi, H. Khurshid, G. H.Warsi, M. Alam, A. Rahim, "Computational Study on the Diffuser of Formula Racing Car." In *Future Learning Aspects of Mechanical Engineering*, 481–496. Singapore: Springer, 2022. https://doi.org/10.1007/978-981-99-1894-2_41

[13] M. Basso, C. Cravero, and D. Marsano. "Aerodynamic Effect of the Gurney Flap on the Front Wing of a F1 Car and Flow Interactions with Car Components." *Energies* 14, no. 8 (2021): 2059. https://doi.org/10.3390/en14082059

[14] S. Upadhye1, D. Khairwa, M. Nagpure, A. Mangrulkar, A. Deotale, H. Nagpure, "Estimation of Drag and Downforces Using Aerodynamic Profile on Formula Student Vehicle." *International Journal of Engineering Research and Technology*, 2021.

[15] J. Katz, et al. "Aerodynamics in Motorsports." *Proceedings of the Institution of Mechanical Engineers, Part P: Journal of Sports Engineering and Technology* 235, no. 4 (2021): 324–338. https://doi.org/10.1177/1754337119893226

[16] C. Cravero, and D. Marsano. "Computational Investigation of the Aerodynamics of a Wheel Installed on a Race Car with a Multi-Element Front Wing." *Fluids* 7, no. 6 (2022): 182. https://doi.org/10.3390/fluids7060182

[17] P. Qin, A. Ricci, and B. Blocken. "CFD Simulation of Aerodynamic Forces on the DrivAer Car Model: Impact of Computational Parameters." *Journal of Wind Engineering and Industrial Aerodynamics* 248 (2024): 105711. https://doi.org/10.1016/j.jweia.2024.105711

[18] M. I. Ma'arof, L. Puvunathan, W, Z, M, Yusof, S. Suresh, G. T. Chala, "Computational Fluid Dynamic (CFD) Analysis to Determine Canard's Downforce." *INTI Journal* 22 (2020).

[19] A. Bhosale, M. S. Malik, S. P. Dillibabu, V. K. Javanjal, R, Karthikeyan K. "Enhancing Passenger Vehicle Performance: A Study of CFD Technique and Machine Learning for Optimal Rear Spoiler Design and Lateral Stability." *International Journal of Intelligent Systems and Applications in Engineering* 12, no. 2 (2024): 100–111.

[20] T. P. O'Driscoll, and A. R. Barron. "CFD Analysis of the Location of a Rear Wing on an Aston Martin DB7 in Order to Optimize Aerodynamics for Motorsports." *Vehicles* 4, no. 2 (2022): 608–620. https://doi.org/10.3390/vehicles4020035

[21] A. Guerrero, R. Castilla, and G. Eid. "A Numerical Aerodynamic Analysis on the Effect of Rear Underbody Diffusers on Road Cars." *Applied Sciences* 12, no. 8 (2022): 3763. https://doi.org/10.3390/app12083763

[22] J. Pacheco, A. C. Marta, and L. Eça. "Wind Tunnel Testing of a Formula Student Vehicle for Checking CFD Simulation Trends." *Proceedings of the Institution of Mechanical Engineers, Part D: Journal of Automobile Engineering* vol. 238, no. 14 (2023). https://doi.org/10.1177/09544070231203076

[23] X. Castro, and Z. A. Rana. "Aerodynamic and Structural Design of a 2022 Formula One Front Wing Assembly." *Fluids* 5, no. 4 (2020): 237. https://doi.org/10.3390/fluids5040237

[24] Predescu, O. G. *Racecar Undertray Study for a Formula SAE Prototype.* Bachelor's thesis, Universitat Politècnica de Catalunya, 2022.

[25] M. Lučić, "Computational Fluid Dynamics (CFD) Analysis of the Divergent Part of the Formula Student Car Restrictor." *Transactions of Motauto World* 8, no. 1 (2023): 9–13.

[26] K. Ambo, H. Nagaoka, D. A. Philips, C. Ivey, G. A. Brès and S. T. Bose, "Aerodynamic Force Prediction of the Laminar to Turbulent Flow Transition Around the Front Bumper of the Vehicle Using Dynamic-Slip Wall Model LES." In *AIAA SciTech 2020 Forum*, 0036, 2020. https://doi.org/10.2514/6.2020-0036

[27] P. Singh, V. Chhettri, and N. K. Gupta. "Computational Analysis of Aerodynamics Characteristics of High-Speed Moving Vehicle." In *Characterization, Testing, Measurement, and Metrology*, 125–137. Boca Raton, FL: CRC Press, 2020.

[28] Y. Indrawan, and M. Mulyadi. "Pengaruh Variasi Model Body Formula SAE terhadap Efisiensi Kerja dengan Uji Simulasi Aerodinamika." *Innovation Technology: Methodical Research Journal* 3, no. 3 (2024): 12. https://doi.org/10.47134/innovative.v3i3.111

[29] Chen, Y., J. Zhou, G. Su, and C. Wang. "Design and Analysis of FSC Formula Racing Car Body." *Journal of Physics: Conference Series* 1635, no. 1 (2020): 012025. https://doi.org/10.1088/1742-6596/1635/1/012025

[30] M. Dickison, M. Ghaleeh, S. Milady, S. Subbakrishna, L. T. Wen, M. Al Qubeissi, "Investigation into the Aerodynamic Performance of a Concept Sports Car." *Journal of Applied Fluid Mechanics* 13, no. 2 (2020): 583–601. https://doi.org/10.29252/jafm.13.02.30179

[31] N. Stojanovic, O. I. Abdullah, Ivan Grujic, Jasna Glisovic, "The Influence of Spoiler on the Aerodynamic Performances and Longitudinal Stability of the Passenger Car Under High-Speed Condition." *Journal of Visualization* 26, no. 1 (2023): 97–112. https://doi.org/10.1007/s12650-022-00867-2

[32] S. Anbalagan, C. Deepak, K. Virmani, and T. Madhogaria. "Computational Analysis of Pitch Sensitivity for Concept Race Cars." *SAE Technical Papers*, (2022).

[33] A. Huminic, and G. Huminic. "Aerodynamic Study of a Generic Car Model with Wheels and Underbody Diffuser." *International Journal of Automotive Technology* 18, no. 3 (2017): 397–404. https://doi.org/10.1007/s12239-017-0040-6

[34] A. Piszczatowski, M. Kmiotek, A. Kordos, and A. Zaremba. "Modeling of the Front Wing Cross-Section for a Formula Student Vehicle." *Advances in Science and Technology Research Journal* 20, no. 6 (2026). https://doi.org/10.12913/22998624/216767

[35] E. N. Hogea, R. J. Hogea, and R. K. Agarwal. "3D Iterative Parametric Optimization Study of a FSAE Aerodynamic Package Using Computational Fluid Dynamics." In *AIAA SciTech 2026 Forum*, 1898, 2026. https://doi.org/10.2514/6.2026-1898

[36] Sankar, Hari, Sarang Holay, Masami Ikeda, and Ramanand Singh. "Understanding Prevailing Physics in Automotive Aerodynamics Applications—Detached Eddy Simulation vs Reynolds-Averaged Navier–Stokes Approach." *SAE International Journal of Commercial Vehicles* 19, no. 4 (2026). https://doi.org/10.4271/02-19-04-0023

[37] C. M. de Freita, G. D. Telli, and J. S. Rosa. "Aerodynamic Influence of Front Wing Geometry on Formula One Car Performance: A Computational Fluid Dynamics Review." In *SAE Brasil 2025 Congress*. SAE Technical Paper, 2025. https://doi.org/10.4271/2025-36-0043